



HAL
open science

Black Holes and Galactic Density Cusps I Radial Orbit Cusps and Bulges

Morgan Le Delliou, Richard Henriksen, Joseph D. Macmillan

► **To cite this version:**

Morgan Le Delliou, Richard Henriksen, Joseph D. Macmillan. Black Holes and Galactic Density Cusps I Radial Orbit Cusps and Bulges. 2010. hal-00431275v5

HAL Id: hal-00431275

<https://hal.science/hal-00431275v5>

Preprint submitted on 11 Nov 2010 (v5), last revised 20 Mar 2011 (v7)

HAL is a multi-disciplinary open access archive for the deposit and dissemination of scientific research documents, whether they are published or not. The documents may come from teaching and research institutions in France or abroad, or from public or private research centers.

L'archive ouverte pluridisciplinaire **HAL**, est destinée au dépôt et à la diffusion de documents scientifiques de niveau recherche, publiés ou non, émanant des établissements d'enseignement et de recherche français ou étrangers, des laboratoires publics ou privés.

Black Holes and Galactic Density Cusps I: Radial Orbit Cusps and Bulges

M. Le Delliou^{1*}, R.N. Henriksen^{2*} and J.D. MacMillan^{3*}

¹*Instituto de Física Teórica UAM/CSIC, Facultad de Ciencias, C-XI, Universidad Autónoma de Madrid Cantoblanco, 28049 Madrid SPAIN*

²*Queen's University, Kingston, Ontario, Canada*

³*Faculty of Science, University of Ontario Institute of Technology, Oshawa, Ontario, Canada L1H 7K4*

Send offprint requests to: MLeD
Submitted ...; Received ...; Accepted...

Preprint: IFT-UAM/CSIC-09-26

ABSTRACT

In this paper we study the distribution functions that arise naturally during self-similar radial infall of collisionless matter. If a rigorous steady state is assumed, then the system is infinite and is described by a universal distribution function for a general self-similar index. The logarithmic potential case is exceptional and yields the familiar Gaussian for an infinite system with an inverse-square density profile. We also show that for time-dependent radial self-similar infall, the logarithmic case is accurately described by the Fridmann and Polyachenko distribution function. The system in this case is finite but growing. We are able to embed a central mass in the universal steady distribution only by iteration except in the case of massless particles. The iteration yields logarithmic corrections to the massless particle case and requires a ‘renormalization’ of the central mass. A central spherical mass may be accurately embedded in the Fridmann and Polyachenko growing distribution however. Some speculation is given concerning the importance of radial collisionless infall in actual galaxy formation.

Key words: Cosmology:theory – Dark Matter – large-scale structure of Universe - Galaxies:formation – galaxies:haloes – galaxies: bulges - gravitation

1 INTRODUCTION

The relation between the formation of black holes and of galaxies has developed into a key astrophysical question. From the early papers by Kormendy and Richstone (Kormendy & Richstone 1995), to the more recent discoveries by Magorrian et al. (Magorrian et al. 1998), Ferrarese and Merritt (Ferrarese & Merritt 2000), and Gebhardt et al. (Gebhardt et al., 2000). These papers establish a strong correlation between what is essentially the black hole mass and the surrounding stellar bulge mass (or velocity dispersion). The origin of this proportionality, which extends well beyond the gravitational dominance of the black hole, remains unproven. But it is generally taken to imply a coeval growth of the black hole and bulge.

Various proposals have been offered to explain the black hole mass-bulge mass proportionality as a consequence of the AGN phase. There is as yet no generally accepted scenario although a kind of ‘auto-levitation’ or feed-back mech-

anism is plausible. In any event there remains the question of the origin of the seed masses. In some galaxies at very high red shift the inferred black hole masses are already of order $10^9 M_\odot$ (Kurk et al., 2007, for e.g.) after about one Ga of cosmic time. This may require frequent, extremely luminous early events (Walter et al., 2009, for e.g.), or it may suggest an alternate growth mechanism.

The latter possibility is reinforced by the detection of a change in the normalization of the black hole mass-bulge mass proportionality in the sense of relatively larger black holes at high red shift (Maiolino et al. 2007, for e.g.). As suggested in that paper it seems that the black holes may grow first, independently of the bulge. The collisionless matter that we invoke might be stars or it might be the dark matter itself.

Recently (Peirani & de Freitas Pacheco 2008) have studied the possible size of the dark matter component in black hole masses. By assuming that the dimensional or ‘pseudo phase space density’ (H2006, i.e. Henriksen 2006b, for e.g.) is strictly constant they convert the relativistic accretion of the dark matter into an adiabatic Bondi flow problem and obtain the resulting accretion rate. Then by adopting the mass proportionality between bulge and black hole and

* Email: Morgan.LeDelliou@uam.es (MLeD); henriksn@astro.queensu.ca (RNH); joseph.macmillan@gmail.com (JDMcM)

fitting boundary conditions from cosmological halo simulations, they deduce that between 1% and 10% of the black hole mass could be due to dark matter.

If we accept this result at face value, it seems that a seed mass of say $10^6 M_\odot$ could have grown from dark matter. It would now be part of a super massive black hole that subsequently grew in the AGN phase. Some seeds may be primordial. As early as 1978 fully general relativistic numerical collapse calculations (Bicknell & Henriksen 1979) predicted primordial black hole masses in the range 10^2 to $10^6 M_\odot$.

In this and subsequent papers we will attempt to embed a black hole (or at least a central mass) in a distribution of particles that arises naturally during the formation of the galactic core. We will predict the consequent density cusp profile and that of the velocity dispersion variation in the cusp. It is perhaps significant in the light of the extensive orbital study of ((Van den Bosch et al. 2008)) that we are most successful in a time-dependent case. For these authors suggest that the central mass may render the orbits chaotic and non-stationary. We find in the steady systems that a series of iterations diverges at the centre.

Density cusps surrounding black holes have been studied extensively previously. Classic studies by (Peebles 1972) and by (Bahcall & Wolf 1976) dealt with the problem of feeding the black hole from a filled loss cone (nearly radial orbits). In addition to these diffusion studies, Young (Young 1980) explored the cusps produced by the adiabatic growth of a black hole in a pre-existing isothermal stellar environment. This was extended by (Quinlan et al 1995) and by (MacMillan & Henriksen 2002) to more general environments. In a cosmological context, Bertschinger (1985) also studied the growth of a central black hole by radial infall. The conclusions were that the black hole induced cusps were never flatter than $r^{-1.5}$ (the isothermal and cosmological case) and that no black hole mass-bulge mass correlation was established (MacMillan & Henriksen 2002). This latter conclusion has spurred the investigation of coeval dynamical growth of the black hole and bulge in contrast to adiabatic growth (MacMillan & Henriksen 2003).

Such concerns have passed from the abstract to the practical with the detection of stellar cusps around galactic nuclear black holes (Gillessen et al., 2009). This latter paper reports stellar cusp power laws for the central Milky Way in the range -1.1 ± 0.3 , significantly shallower than the adiabatic -1.5 or the zero flux (Bahcall & Wolf 1976) -1.75 . We seek to find under what general conditions such power laws may arise during collisionless infall. In the present paper that is restricted to radial infall, we do not find cusps flatter than r^{-2} .

An effective alternate method of evolving flat cusps is to invoke tight binary black hole systems produced by mergers that 'scour' the stellar environment (Merritt & Szell 2006; Nakano & Makino 1999, for e.g.). Depending on the power law assumed for the initial stellar environment, Merritt and Szell simulate scoured power laws that can be as flat as -1 in an initially -1.5 cusp, and as flat as -0.5 in an initially -1 stellar cusp. Flatter values are reduced to essentially constant density cores. The -1 slope as noted above is a reasonable fit to the Milky Way (ibid).

Subsequently, but taking at least the central relaxation time, the cusps should regenerate to the zero flux condi-

tion ($r^{-1.75}$) according to the simulations in (Merritt & Szell 2006). However this will extend only out to about 0.2 of the gravitational influence radius of the black hole. This regeneration is not thought to be relevant to the Milky Way central stellar cusp, but may be present on small scales elsewhere.

Such a picture is seductive, especially given the recent detection of a strong correlation between the nuclear black hole mass and the central luminosity deficit (Kormendy & Bender 2009). However the correlation in itself only implicates the influence of the black hole. It does not necessarily require the merger history, which in any case is unlikely to be the same for different galaxies. Consequently we explore in this series of papers (I; II; III) whether cusps as flat as those resulting from scouring might also be produced during the dynamical formation of the black hole or mass concentration. In this first paper we present a summary of the situation for radial orbits since the arguments are typical but easily carried out in that case.

The first general result on radial infall was in fact given in (Fillmore & Goldreich, 1984) and the Bertschinger (1985) result follows by putting their parameter $\epsilon_{FG} = 1/3$. However neither this work nor that of Bertschinger attempted to infer closed forms for the equilibrium distribution function. This was begun by Henriksen and Widrow in 1995. In (H2006) it is pointed out that $a = 9/8$ ($\epsilon = 3$) yields the Bertschinger solution in its entirety, including the recently heralded power law of the proxy for phase space density. The parameter $\epsilon = 3\epsilon_{FG}$ and it is related to the index called 'a', both by simulations and theory.

We are aware that such a radial system is unstable to the radial orbit instability on small scales (MWH 2006, coined ROI). However even fully cosmological simulations show an outer envelope wherein the orbits are trending to be radial. Moreover isolated halos, which also show statistical relaxation that is begging to be understood, show quite radial orbits in the envelope (ibid). We speculate below that the growth of the bulge in such an envelope may be described in terms of radial infall, and that this might continue hierarchically to smaller scales after relaxation by the ROI and clump-clump interactions (MacMillan & Henriksen 2003). Such interactions would remove angular momentum from some particles in favour of others.

We begin the next section with the general formulation in spherical symmetry. Subsequently we discuss the various possible steady distribution functions (DF from now on) for radial orbits. Then we show that the DF of Fridman and Polyachenko (Fridmann & Polyachenko 1984, hereafter called FPDF) describes a system of radial orbits that is growing self-similarly. This is contrasted with an infinite steady system for which the DF is Gaussian. After some discussion, we give our conclusions.

2 DYNAMICAL EQUATIONS IN INFALL VARIABLES

Following the formulation of (H2006) in this section we transform the collisionless Boltzmann and Poisson equations to 'infall variables'. We treat a spherically symmetric anisotropic system in the 'Fujiwara' form (Fujiwara 1983, for e.g.) namely

$$\frac{\partial f}{\partial t} + v_r \frac{\partial f}{\partial r} + \left(\frac{j^2}{r^3} - \frac{\partial \Phi}{\partial r} \right) \frac{\partial f}{\partial v_r} = 0, \quad (1)$$

$$\frac{\partial}{\partial r} \left(r^2 \frac{\partial \Phi}{\partial r} \right) = 4\pi^2 G \int f(r, v_r, j^2) dv_r dj^2, \quad (2)$$

where f is the phase-space mass density, Φ is the ‘mean’ field gravitational potential, j^2 is the square of the specific angular momentum and other notation is more or less standard.

The ‘infall variables’ are a system of variables and coordinates that allows us either to readily take the self-similar limit or to retain a memory of previous self-similar dynamical relaxation into a true steady state. In this way we can remain ‘close’ to self-similarity just as the simulations appear to do. These coordinates (H2006; H2006A) allow the general expression of the Vlasov-Poisson set, but they also contain a parameter (a) that reflects underlying self-similarity. The self-similar limit is taken by assuming what we term ‘self-similar virialisation’, wherein the system is steady in these coordinates, although it is not absolutely steady since mass is accumulating in this mode.

The transformation to infall variables has the form (H2006, for e.g.)

$$\begin{aligned} R &= r e^{-\alpha T/a}, & Y &= v_r e^{-(1/a-1)\alpha T}, \\ Z &= j^2 e^{-(4/a-2)\alpha T}, & e^{\alpha T} &= \alpha t, \\ P(R, Y, Z; T) &= e^{(3/a-1)\alpha T} \pi f(r, v_r, j^2; t), \\ \Psi(R; T) &= e^{-2(1/a-1)\alpha T} \Phi(r), \\ \Theta(R; T) &= \rho(r, t) e^{2\alpha T}. \end{aligned} \quad (3)$$

This transformation is inspired by the nature of self-similarity, which can be understood as a scaling group wherein each quantity scales according to its dimensions (Carter & Henriksen, 1991). The group parameter is the logarithmic time T . The combinations of scaling constants (note that $a \equiv \alpha/\delta$ see below) multiplying αT in the exponential factor of each physical quantity reflect the dimensions of that quantity. When the dependence on the parameter T is retained in the new variables, there is clearly no invariance along the scaling group motion and so no self-similarity. This means that the passage to the self-similar limit requires taking $\partial_T = 0$ when acting on the transformed variables. Thus the self-similar limit is a stationary system in these variables, which is a state that we have described elsewhere as ‘self-similar virialisation’ (HW 1999; Le Delliou 2001, i.e. Henriksen & Widrow 1999). The virial ratio $2K/|W|$ is a constant in this state (although greater than one; K is kinetic energy and W is potential), but the system is not steady in physical, i.e. untransformed, variables, since infall continues.

The single constant quantity a is the constant that determines the dynamical similarity, called the self-similar index. It is composed of two separate scalings, α in time and δ in space, in the form $a \equiv \alpha/\delta$. The dimensions of any mechanical quantity can be expressed in the scaling space $\vec{a} \equiv (\alpha, \delta, \mu)$, where μ is the mass scaling. The exponential factor of any physical quantity Q (which includes physical constants) is calculated as $\vec{a} \cdot \vec{d}_Q$ where \vec{d}_Q describes the quantity Q in scaling space. Thus for the velocity $\vec{d}_v = (-1, 1, 0)$, for the distribution function $\vec{d}_f = (3, -6, 1)$

and for Newton’s constant $\vec{d}_G = (-2, 3, -1)$. In a gravitation problem the scalings α and δ can express the scalings of all physical quantities having mass, length and time dimensions. This is because we require G to be constant under the scaling motion so that $\vec{a} \cdot \vec{d}_G = 0$ and hence $\mu = 3\delta - 2\alpha$. This changes \vec{d}_f to $(1, -3)$ as used in equation (3). This procedure yields the constants in the exponential factors transforming all physical quantities in the equations (3).

We assume that time, radius, velocity and density are measured in fiducial units $r_o/v_o, r_o, v_o$ and ρ_o respectively. The unit of the distribution function is f_o and that of the potential is v_o^2 . We remove constants from the transformed equations by taking

$$f_o = \rho_o/v_o^3, \quad v_o^2 = 4\pi G \rho_o r_o^2. \quad (4)$$

These transformations convert equations (1),(2) to the respective forms

$$\begin{aligned} &\frac{1}{\alpha} \partial_T P - (3/a - 1)P + \left(\frac{Y}{\alpha} - \frac{R}{a} \right) \partial_R P \\ &- \left((1/a - 1)Y + \frac{1}{\alpha} \left(\frac{\partial \Psi}{\partial R} - \frac{Z}{R^3} \right) \right) \partial_Y P - (4/a - 2)Z \partial_Z P = 0 \end{aligned} \quad (5)$$

and

$$\frac{1}{R^2} \frac{\partial}{\partial R} \left(R^2 \frac{\partial \Psi}{\partial R} \right) = \Theta. \quad (6)$$

This integro-differential system is closed by

$$\Theta = \frac{1}{R^2} \int P dY dZ. \quad (7)$$

Until we enforce the self-similar limit ($\partial/\partial T = 0$) these equations remain completely general, because we have made a continuous and invertible change of variables in equation (3). The merit of the transformation at this stage is only that it puts the expected asymptotic self-similar behaviour in the explicit exponential factors, while relegating the declining time dependence leading to this state to the transformed variables. These variables are strictly independent of T in the self-similar state.

We will in this paper restrict ourselves to the filled loss cone limit of radial infall (HLeD 2002), although this is not the case in subsequent papers of this series. This special case is certainly not realistic where angular momentum becomes important, but it may have application on large scales and in the subsequent evolution in regions where angular momentum is transformed away either by bars or other asymmetries. It may in any case be regarded as an introduction to our methods.

To proceed we set

$$P = F(R, Y; T) \delta(Z) = F(R, Y; T) \delta(j^2) (e^{(4/a-2)\alpha T})$$

($\delta()$ is the Dirac delta, not the scaling delta) which changes the scaling for the DF in equation (3) to

$$\pi f = F(R, Y; T) e^{(1/a-1)\alpha T} \delta(j^2), \quad (8)$$

while other scalings remain unchanged.

The governing equations now become equation (6) plus the Boltzmann equation for $F(R, Y; T)$ in the form

$$\frac{1}{\alpha}\partial_T F + (1/a - 1)F + \left(\frac{Y}{\alpha} - \frac{R}{a}\right)\partial_R F - \left((1/a - 1)Y + \frac{1}{\alpha}\frac{\partial\Psi}{\partial R}\right)\partial_Y F = 0. \quad (9)$$

Finally equation (7) reduces to

$$\Theta = \frac{1}{R^2} \int F dY. \quad (10)$$

This completes the formalism that we will use to obtain the results below.

3 STEADY CUSPS AND BULGES WITH RADIAL ORBITS

We expect one mode of relaxation in collisionless cusps to be of the ‘moderately violent’ type satisfying, in terms of the particle energy E and mean field potential Φ , the relation

$$\frac{dE}{dt} = \frac{\partial\Phi}{\partial t}|_r. \quad (11)$$

This includes phase-mixing. Another mode (Diemand et al., 2006) is furnished by the presence of hierarchical sub-structure. The sub-structure can interact in clump-clump interactions that can induce relaxation on a coarse-grained scale (H2009, i.e. Henriksen 2009).

However the temporal evolution of the system is difficult to follow analytically even in the self-similar limit, so we normally look for equilibria established by the evolution. This may be either a strictly steady state in some appropriate coarse-grained description, or it may be a self-similar virialised state.

In general one can not find a unique solution of the governing equations that consistently reproduce infall onto a central mass. We find that this is possible in one interesting case (Fridman and Polyachenko DF) of accretion onto a point mass, but not for a truly steady distribution around a point mass. One can allow for the presence of a point mass in a steady distribution by iterating about an equilibrium state that is determined initially by the central mass. This allows the central mass and the environment to be evolved together towards a new equilibrium, although normally only a single loop is feasible. We proceed to discuss these two possibilities in this section.

Using the characteristics of equation (9) plus the total derivative

$$\frac{d\Psi}{ds} = \frac{\partial\Psi}{\partial s} + \frac{dR}{ds}\partial_R\Psi \quad (12)$$

where $ds \equiv \alpha dT$, one finds by a simple manipulation that

$$\frac{d(\frac{Y^2}{2} + \Psi)}{ds} = -2(1/a - 1)\frac{Y^2}{2} - \frac{R}{a}\partial_R\Psi + \frac{\partial\Psi}{\partial s}. \quad (13)$$

In order for this last equation to yield the energy as an isolating integral (i.e. characteristic constant) the last two terms must together sum to give $-2(1/a - 1)\Psi$. This is most simply effected by setting $\partial\Psi/\partial s = 0$ and $R\partial_R\Psi = p\Psi$, which turns out to be a condition for both self-similarity and a **true** steady state. Here

$$p = 2(1 - a). \quad (14)$$

so that $\Psi = \Psi_o R^p$ for some constant Ψ_o .

Hence, on setting $\mathcal{E} \equiv Y^2/2 + \Psi$, we have from equation (13)

$$\frac{d\mathcal{E}}{ds} = -2(1/a - 1)\mathcal{E}. \quad (15)$$

This variation does render E constant on characteristics (and therefore in time) as one sees by integrating to the form $E_o \exp(-2(1/a - 1)s)$, and then by using the transformations (3) to find $E = \mathcal{E} \exp(2(1/a - 1)\alpha T) \equiv E_o$. An example of such a state is a system of massless particles dominated by the potential of a central point mass M_* , for which $a = 3/2$ and $p = -1$. The similarity index $a = 3/2$ reflects the presence of the Keplerian constant GM_* whose vector $\vec{d}_K = (-2, 3)$ and for which $\vec{a} \cdot \vec{d}_K = 0$. We refer to this example again below.

Equation (9) also yields along the characteristic

$$\frac{dF}{ds} = -(1/a - 1)F, \quad (16)$$

so that with equation (15)

$$F = \tilde{F}(\kappa)|\mathcal{E}|^{1/2}. \quad (17)$$

The steady unscaled DF follows from this last equation and the transformations (3) as ($a \neq 1$)

$$\pi f = \tilde{F}(\kappa)|E|^{1/2}\delta(j^2). \quad (18)$$

The quantity κ in equation (18) labels any *other* (besides E) possible characteristic constant, but in general nothing other than E is readily available. For this reason we discuss the DF (18) with \tilde{F} strictly constant.

In (HW95) this DF was first given and was shown to yield the asymptotic particle distribution found by Fillmore and Goldreich (Fillmore & Goldreich, 1984). Their result followed from a direct integration of particle orbits in radial infall. The example given in (HW95) for comparison purposes corresponds to the choice of our current index $a = 18/17$. In general, $a = 3\epsilon/2(\epsilon + 1)$, where the initial density profile is $\propto r^{-\epsilon}$. The initial system is infinite for $\epsilon \leq 3$, which is $a \leq 9/8$. In (HW 1999) this DF was argued to be the natural state for steady self-similarity. Thus the DF (18) with \tilde{F} constant probably describes a steady system of self-similar radial orbits characterized by the index a . For this reason together with the numerical evidence discussed presently, we discuss the implications here in more detail, bearing in mind the possibility of embedding a central black hole.

In (HW 1999) weak evidence was presented to show that the $|E|^{1/2}$ law did appear near the end of the infall for the most tightly bound particles. These would be closest to being described as occupying an eternal steady state. A similar result was found by MacMillan (MacMillan 2006) for the most tightly bound particles even while infall continued. The case was re-enforced by additional calculation of initially infinite systems by Le Delliou (Le Delliou 2001) (see figure 1). The figure shows another example of the Fillmore and Goldreich (ibid) problem wherein the DF (18) is a reasonable fit over most of the energy range. The cut-off is probably numerical in this case since numerically the system is ultimately finite.

However the DF (18) does *not* fit the complete energy distribution found in high resolution simulations of radial orbit *growing* isolated halos (MacMillan 2006, for e.g.) in a

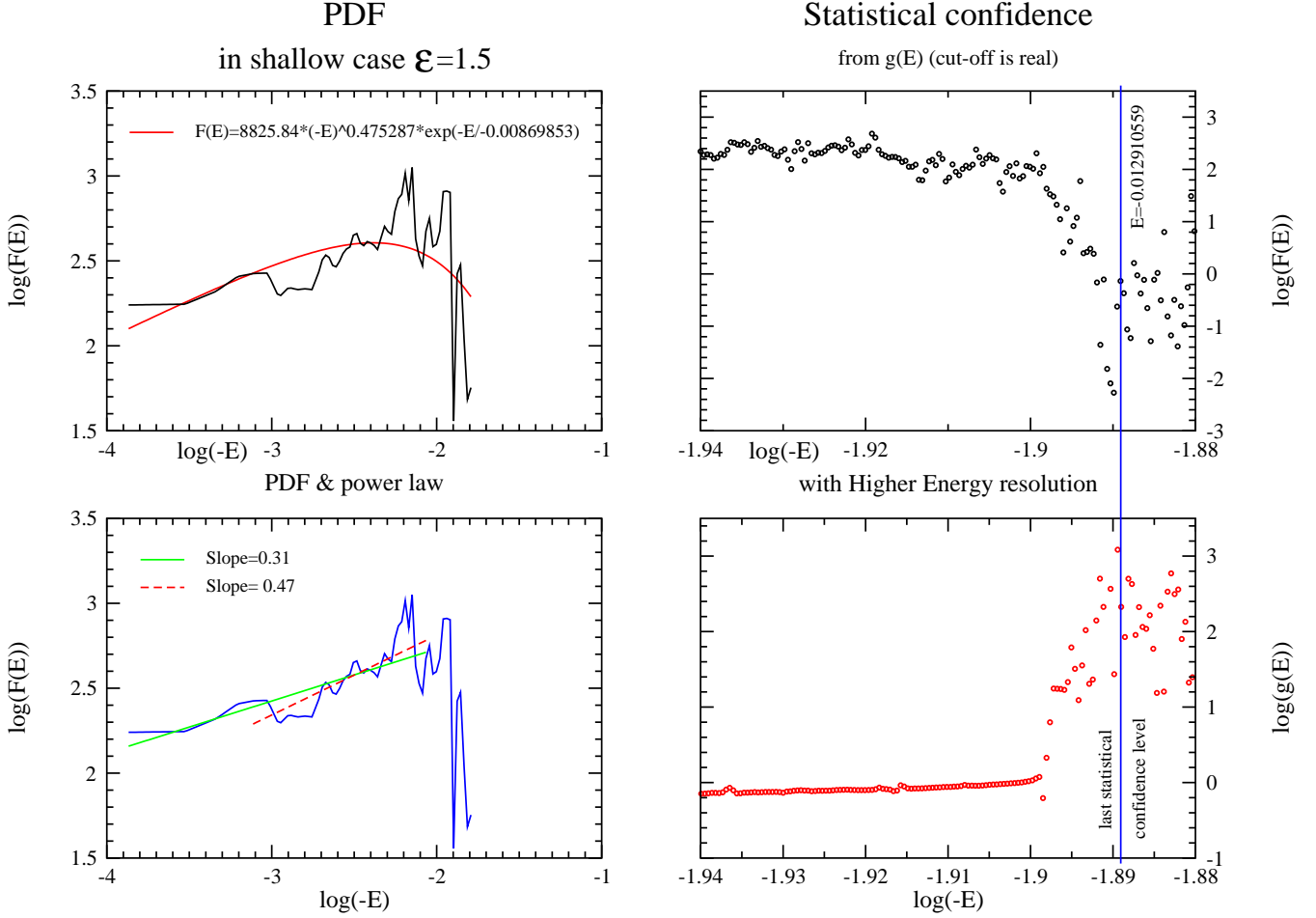


Figure 1. A shell code evaluation of the DF (Le Delliou 2001), evolved from a system with initial density $\rho \propto r^{-1.5}$. The first fit is with a cut off power law ($F \propto E^{-p} e^{-E/E_c}$ with $p \simeq 1/2$, $E_c \simeq -10^{-2}$; upper left panel), while the second fit is just a power law (lower left), confirming (HW99). The cut off is confirmed by higher resolution in the DF (upper right) and in density of states $g(E)$ (lower right).

state of self-similar virialisation (HW 1999). In such a state, infall continues. We reserve the explanation of this behaviour to the next section where it involves the exceptional case wherein $a = 1$.

Continuing for the moment with the discussion of equation (18) we observe that an upper energy cut-off $E_+ \propto \Phi$ is required for finiteness in the positive energy case ($a < 1$ when the potential increases outwards), while the cut-off is zero in the negative energy case ($a > 1$ when the potential decreases outwards). Moreover we note that one can add an arbitrary constant E_o to E in this DF, which reflects the arbitrary constant in the potential. For negative energy the DF would appear as $\tilde{F}(E_o - E)^{1/2}$ for $E < E_o < 0$. This was the type of fit used by MacMillan (ibid) to fit his simulations. The DF decreases to zero at E_o and increases to negative energy. A large positive constant E_o and $E > -E_o$ so that $f \propto (E_o + E)^{1/2}$ would express a negative energy cut-off at the value $-E_o$ and the DF would increase towards zero energy.

The potential and density pair for these eternally steady models take the form¹ ($a \neq 1$)

$$\Psi = \Psi_o R^{(2-2a)}, \quad \Theta = 2(3 - 2a)(1 - a)\Psi_o R^{-2a}. \quad (19)$$

In a very recent submission Amorisco and Evans (Amorisco&Evans 2010) prove that the power-law relation between the galactic half-light radius and the central velocity dispersion in dwarf ellipticals requires a power law potential to be valid. This arises naturally here.

In the example of a dominant central point mass, inserting the index $a = 3/2$ in the above pair yields a point mass surrounded by massless particles. The massless particles may be distributed in any manner, but since $\vec{d}_N = (0, -3)$ dimensional analysis requires that the number density N should vary as $N \propto N_o(R)e^{-3\delta r} = N_o(R)R^3/r^3$. In a rigorously steady state this should be time independent so that $N_o(R) \propto R^{-3}$ and hence $N \propto r^{-3}$. Such a halo could exist outside any dominant mass as was discussed in (HW 1999). Thus it might surround a central point mass or indeed be the diffuse halo around a bulge containing most of the system mass. However this is only a limiting behaviour

previous papers, in which δ, X, S in ((HW 1999)) are respectively $1/a, R, \Theta R^2$. In ((HW95)) δ there becomes $1/(1 - a)$ in current notation.

¹ We have used our current notation when using the results of

and does not include the transition region. This interests us particularly in the context of central black holes.

The direct density integral over the DF (18) for negative energies yields for ρ

$$\rho = \frac{\pi \tilde{F} |\Phi|}{\sqrt{2} r^2}. \quad (20)$$

Since this is linear in the potential, one can readily include a central mass by iteration. We may begin with a point mass potential for Φ in the density (20), and then use the Poisson equation to obtain a new potential in a form that is no longer self-similar. This yields

$$\Phi_1 = -\frac{M_* + C_2(1 + \ln r)}{r}, \quad (21)$$

whence follows a new density by (20). The constant M_* would be the mass **inside** $\ln r = -1$ (regarded as a point mass) while $C_2 = (\pi \tilde{F} / \sqrt{2}) M_*$. There is only a logarithmic modification to the r^{-3} law at large r where the iteration should apply. In effect the iteration yields a singular perturbation series at $r = 0$ because of the diverging potential and hence energy. Therefore we arbitrarily cut off the series at small r and ‘renormalize’ the central mass. The next loop of the iteration gives

$$\Phi_2 = -\frac{M_*(1 - \frac{C_2^2}{2M_*^2})}{r} - C_2(1 + \frac{2C_2}{M_*})\frac{(1 + \ln r)}{r} - \frac{\ln^2 r}{r} \frac{C_2^2}{2M_*}$$

where again we have ‘renormalised’ at $\ln r = -1$. Putting this back into equation (20) yields ρ_2 as r^{-3} flattened only by logarithmic terms at large r (HW 1999). The large scale r^{-3} density profile does not fit the bulge simulations inside the NFW (Navarro, Frenk & White 1996) scale length, but it does describe the halo region outside a central bulge of mass M_* (HW 1999).

Since the density is linear in the potential we may also solve for a self-consistent cusp having the DF (18) by letting the potential be determined by the Poisson equation. Working in transformed variables we find

$$\Psi = -AR^{p_-} - BR^{p_+}, \quad (22)$$

where A, B are arbitrary real constants > 0 and

$$p_{\pm} = -\frac{1}{2} \pm \sqrt{\frac{1}{4} - \frac{\pi}{\sqrt{2}} \tilde{F}}. \quad (23)$$

By letting $\tilde{F} \rightarrow 0$ we see that p_- is the power that should be taken near the centre if we wish to create a strong central mass concentration. It tends to -1 in this limit while p_+ tends to zero. Hence we set $B = 0$ in this limiting domain. The potential then satisfies our basic condition (14) with a new self-similar index. This is given by $a = 1 - p_-/2$ according to equation (14), that is explicitly

$$a_- = \frac{5}{4} + \frac{1}{2} \sqrt{\frac{1}{4} - \frac{\pi}{\sqrt{2}} \tilde{F}}. \quad (24)$$

Equation (19) now gives the inner cusp density law as

$$\Theta = |p_-|(1 + p_-)|\Psi_o|R^{(-2+p_-)}. \quad (25)$$

This can not be flatter than $R^{-2.5}$, which appears only for the ‘maximum bulge’ for which $\tilde{F} = 1/(2\pi\sqrt{2})$. At large r

the term in p_+ dominates, and the behaviour tends to r^{-2} for \tilde{F} small.

In the context of dark matter simulations such a steady halo of radial orbits could describe the region just beyond the NFW scale radius, based on the density profile alone. It is not stable in a strict steady state according to the usual Antonov criteria (Binney & Tremaine 1987, for e.g.), unless the energy is negative. Consequently we do not expect it in central regions where $a < 1$ where the energy is positive (with a central zero: the potential increases outward according to Eq. 19). The radial velocity dispersion is $\overline{v_r^2} = |\Phi|/2$.

This concludes our study of the general, steady, spherically symmetric, DF for power law distributions of radial orbits. The main justification for the study is that it permits definite conclusions. The effect of an embedded mass is more problematic, but iteration does suggest the r^{-3} law to within logarithmic corrections.

In the next section we turn to the exceptional case for which $a = 1$. We are able to place this case in the context of other discussions.

4 THE LOGARITHMIC CASE

The case $a = 1$ is obviously special and, as it turns out, rather important. We return to the equation (13) and observe that we also have an integral in the steady state if $\psi = \psi_o \ln R$. For in that case the equation integrates to $\mathcal{E} + \psi_o \alpha T = \kappa$, where κ is constant on the characteristic. Equation (16) then requires that in general $F = F(\kappa)$, so F is also constant on the characteristic. With $a = 1$ we note from equation (3) that $\Psi \equiv \Phi$, $Y \equiv v_r$, and so $\mathcal{E} \equiv E$. However $\kappa = v_r^2/2 + \psi_o \ln R + \alpha T = v_r^2/2 + \psi_o \ln r \equiv E$ and moreover $\pi f \equiv F$. Hence our conclusion is for the moment only that

$$\pi f = F(E), \quad (26)$$

in this case.

By taking the potential to be logarithmic $\Psi = \Psi_o \ln R$, we have required by equation (6) that $\Theta = \Psi_o/R^2$ and hence, by the appropriate members of the set (3), that $\rho = \Psi_o/r^2$. But for consistency we must also have

$$\rho = \frac{\Psi_o}{r^2} = \frac{1}{r^2} \int F(E) dv_r. \quad (27)$$

We must therefore find a DF $F(E)$ which satisfies this equation. In effect, the integral over the particle velocities must be a constant independent of the logarithmic potential.

To find such a DF we convert the integral to an integral over energy in the normal fashion and write our consistency condition as

$$I \equiv \sqrt{2} \int \frac{F(E)}{\sqrt{(E - \Phi)}} dE = \Psi_o. \quad (28)$$

We might expect a power law form for $F(E)$ on general grounds, and given this a brief experimentation shows that the most general form for $F(E)$ in this case may be written as (we suppose negative energy to ensure convergence and $E < E_o < 0$ where E_o is an arbitrary constant energy)

$$F(E) = \frac{K}{\sqrt{(E_o - E)}} \quad (29)$$

This may also be inferred as the unique solution with a finite energy range by recognizing that equation (28) is really a simple form of Abel's integral equation (see e.g. (Binney & Tremaine 1987) in the first or finite form, p651) whose solution is equation (29) with

$$K = \frac{\Psi_o}{\sqrt{2\pi}}. \quad (30)$$

This may be checked by direct evaluation of the integral to find that $\rho = \Psi_o/r^2$ as required.

This result holds only where $E < 0$ and hence where $r < r_o$, where r_o is an arbitrary scale. However since we have not actually set a fixed scale in the problem (which would entail setting $\delta = 0$), we have implicitly implied that $r/r_o = R/R_o$. Thus we have assumed that $r_o = R_o e^{\alpha T} = \alpha R_o t$. We may take R_o constant (dimensionless) so that there is a residual time dependence because the outer boundary expands according to $r_o = R_o e^{\alpha T}$. This implies that the mass inside R_o and indeed inside any fixed R is growing as $M = 4\pi\Psi_o R \alpha t$.

We have thus succeeded according to the above in deriving the Fridman and Polyachenko DF (Fridman & Polyachenko 1984) as the unique result of time-dependent radial accretion of a growing inverse-square density 'bulge'. This is one of our major conclusions.

A numerical measure of the DF in radial self-similar continuing infall was made by MacMillan (MacMillan 2006). Instead of the steady DF, the DF of Fridman and Polyachenko (Fridman & Polyachenko 1984) is found to predict accurately all of the measured quantities as in the accompanying figures. These include an inverse square density law and a power law pseudo phase space density of ≈ -1.5 , but there are logarithmic corrections to the power law as can be calculated from the FP distribution function. The pseudo phase space density power is flatter (MWH 2006, i.e. MacMillan, Widrow & Henriksen 2006) than is generally found in full cosmological simulations. These results are illustrated in figures (2) and (3).

This DF (Fridman & Polyachenko 1984) used to make the fits in figures (2) and (3) is

$$f = \frac{K}{(-E + E_o)^{1/2}} \delta(j^2), \quad (31)$$

for $E < E_o \leq 0$, and $r \leq r_f$ (where $\Phi(r_f) = E_o$) and zero otherwise. This is just as we inferred above. The density profile is r^{-2} and the potential is logarithmic. The logarithmic variation of the velocity dispersion together with the inverse square density profile accounts for the pseudo density approximate power law found in the simulations (MacMillan 2006).

The persistence of this DF is undoubtedly due to the strict proscription of non-radial forces in the simulations. It is not linearly stable by the Antonov criteria for $E < 0$. When this proscription is relaxed (MacMillan 2006) shows that the equilibrium Fridman and Polyachenko DF is subject to the radial orbit instability. It may require continual non-equilibrium excitation as provided by steady infall to be realized.

The unique feature of the distribution function (31) is that the density is independent of the potential. Hence one can simply add a point mass potential to the logarithmic bulge value and the density will remain $\Psi_o r^{-2}$. In the case of a true absorbing central black hole one should only permit

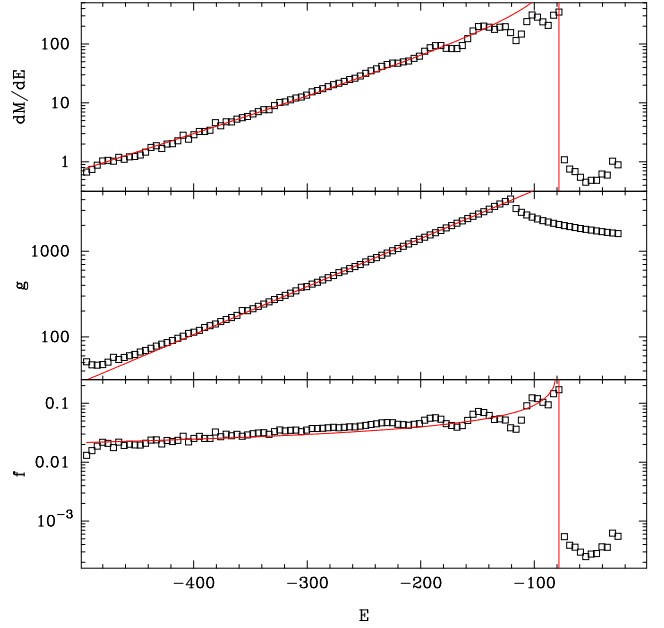


Figure 2. We show the Fridman and Polyachenko fit to the mass distribution $dM/dE = f(E).g(E)$, density of states $g(E)$, and the phase space distribution function $f(E)$. The figure is based on the radial simulations of an isolated dark matter halo by MacMillan (2006). The system is maintained in self-similar virialisation by steady accretion. The fits use equation (31) with $K = -E_o/(4\sqrt{2\pi^3})$ and $E_o \approx -80$ in machine units.

negative radial velocities in the system. This means that K in equation (30) should be multiplied by a factor 2. The velocity dispersion however goes as $\overline{v_r^2} = |\Phi - E_o|$ and we may take $\Phi = -M_*/r + \sqrt{2\pi}K \ln r + E_o$. MacMillan (ibid) finds a good fit to this radial dispersion in his simulations, but without a central mass.

The actual growth of the black hole mass will be simply that of the general self-similar mass growth as discussed above. That is

$$M_*(t) = M_*(0)e^{\alpha T} = M_*(0)\alpha t. \quad (32)$$

Its radius will be growing according to the same law.

One can not however take seriously the growth of a black hole due to radially infalling material from cosmological distances, since the material there can not know the actual location of the black hole. However, as we will speculate in the discussion section, such growth may apply to a hierarchy of 'central' masses extending to ever smaller scales. That is M_* might be successively the bulge of a galaxy, the core, the nucleus, and so on to the black hole. In each case there must be a way of scattering orbits into the essentially radial loss cone.

It is worth contrasting the above infall DF with the eternally steady system of radial orbits in spherical symmetry. This case was inadvertently omitted in (HW95), and so we pause to present it in our general style.

The main difference with the time dependent case is that that the scaling motion must be taken in space rather than in time. This means that we use the variable R , where $e^{\delta R} \equiv \delta r$ so that $dR/dr = e^{-\delta R}$. In addition we write

$$f = F\delta(v_\theta)\delta(v_\phi), \quad (33)$$

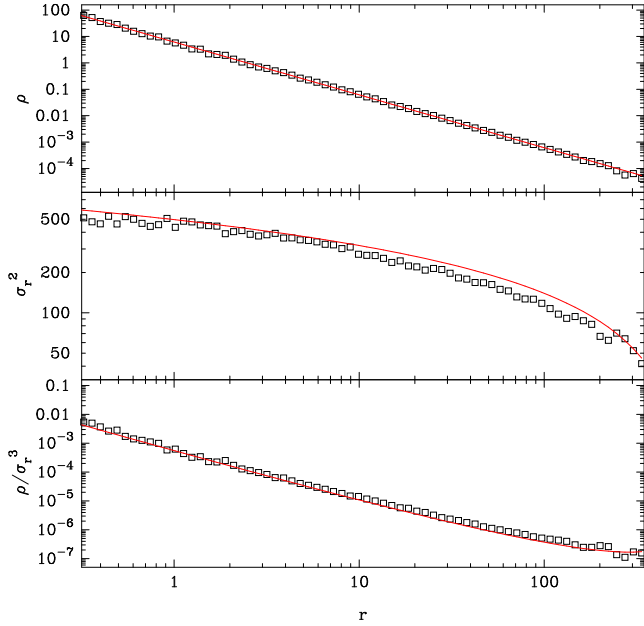


Figure 3. We show the the Fridman and Polyachenko fit to the mass density, the velocity dispersion and the ‘pseudo phase space density’ for the same simulations by MacMillan.

where F satisfies (integrate the steady equation (1) over v_θ and v_ϕ)

$$v_r \frac{\partial F}{\partial r} - \frac{\partial \Phi}{\partial r} \frac{\partial F}{\partial v_r} = 0. \quad (34)$$

In addition we have the Poisson equation as

$$\frac{1}{r^2} \left(\frac{d}{dr} \left(r^2 \frac{d\Phi}{dr} \right) \right) = \rho = \int F dv_r. \quad (35)$$

The dimension vectors in our usual scaling space are $\vec{d}_F = (1, -4, 1)$, $\vec{d}_v = (-1, 1, 0)$, $\vec{d}_\rho = (0, -3, 1)$ and $\vec{d}_\Phi = (-2, 2, 0)$. Recalling that $\mu = 3\delta - 2\alpha$ the vector for F becomes $(-1, -1)$, the vector for ρ becomes $(-2, 0)$ while the others remain unchanged in the reduced (α, δ) space. However we will only consider the case $a = 1$ or $\alpha = \delta$ since the other cases were discussed in (HW95) and reduce to the DF (18). When $\alpha = \delta$ the dimension vectors reduce in delta dimension space to (-2) , (-2) , (0) and (0) respectively. Hence the equivalent of equation (3) is

$$\begin{aligned} \delta r &= e^{\delta R}, & Y &= v_r, \\ e^{-2\delta R} P(R, Y) &= f(r, v_r), \\ \Psi(R) &= \Phi(r, t), \\ e^{-2\delta R} \Theta(R) &= \rho(r). \end{aligned} \quad (36)$$

If self-similarity is enforced normally, then in this case $\partial_R = 0$ when it acts on the scaled variables. However this can not apply to $\Psi(R) = \Phi$ since then equation (34) becomes trivial. The answer lies in the realization that in this case the potential is logarithmic in r , rather than being a power law. The condition $\alpha = \delta$ requires that there be a constant Ψ_o with dimensions of the potential, just as in the time dependent case. These conditions are satisfied here by setting

$$\Psi(R) = \Psi_o(\delta R) \equiv \Psi_o \ln \delta r = \Phi(r).$$

Since only $\partial_R \Psi$ appears in the problem, the self-similar requirement of independence of R is maintained for F .

A direct substitution of the transformation (36) plus the form of the potential into equation (34) reduces it to

$$\frac{1}{P} \frac{dP}{dY} = -\frac{2Y}{\Psi_o},$$

and hence

$$P = K e^{-\frac{Y^2}{\Psi_o}}.$$

Consequently we find finally from $F = P e^{-2\delta R} \equiv P/(\delta r)^2$ the eternally steady DF in the Gaussian form

$$F = K e^{-\frac{2E}{\Psi_o}}, \quad (37)$$

where

$$E \equiv \frac{v_r^2}{2} + \Psi_o \ln \delta r.$$

From the Poisson equation (35) we obtain

$$\rho = \frac{\Psi_o}{r^2},$$

and this must agree with the integral over F . The system is infinite and letting both inward and outward going particles be present one finds that

$$\rho = \frac{K \sqrt{\Psi_o \pi}}{\delta^2 r^2}.$$

Thus

$$K = \sqrt{\frac{\Psi_o}{\pi}},$$

and there would be a factor two on the right if only inward (or less likely) outward going particles were present.

Such behaviour has been found previously as the steady, coarse-grained limit both in spherical symmetry and in arbitrary symmetry (H2004; Lynden-Bell 1967). It is important to note that unlike the time-dependent result, this eternally steady system is infinite in space and in mass. The Fridmann-Polyachenko DF found for the time-dependent infall system, gives a finite although growing mass. Hence it removes one objection to the Gaussian DF for radial orbits. The contrast between the two solutions emphasizes the difference between the completely relaxed DF in the steady state (18) and the DF that is maintained by continuing infall (31).

5 DISCUSSION

In our section on the steady state we have found the the steady, spherically symmetric DF with radial orbits that yields infinite systems with power law profiles. This was found previously but we have attempted to perturb the DF by embedding a central mass. The DF is universal for these systems but the potential-density pair depends on the self-similar index a which in turn depends on dominant constants or boundary conditions. If it is a memory of a cosmological fluctuation profile, then $a = 3\epsilon/(2(\epsilon + 1))$.

The iteration for an embedded central mass predicts a transition region in the halo of the mass that is an r^{-3} profile

modified by logarithmic corrections. It does not correspond to the power law density of stars found close to the black hole in the galactic centre (Gillessen et al., 2009), but may apply in the halo of a bulge mass.

We also looked for solution that broke the self-similarity by seeking non-power-law solutions of Poisson’s equation (pure power laws only exist in the limits) with the density (20). The density profile can not be flatter than $r^{-2.5}$ near a central point mass, but it may be as flat as r^{-2} at large scales in the low density limit.

In the section concerning the logarithmic exception we showed that it corresponded to continuing time-dependent infall. We found both theoretically and numerically that the Fridmann and Polyachenko DF is the distribution established by continuing radial infall. Remarkably, it allows a growing central point mass (or indeed a bulge mass on a larger scale) to be embedded in the infall self-consistently. We were able to contrast this result with an eternally steady, infinite system of radial orbits. This is described by the Gaussian DF that has also been inferred in the past for fully relaxed, infinite systems. In both the steady and the time-dependent cases the density profile is r^{-2} , but a black hole is not readily incorporated into the steady case even by iteration. The time-dependent logarithmic case allows a consistent calculation of the central mass growth rate according to $M_* \propto t$. Such a growth rate from a surrounding envelope was found in (MacMillan & Henriksen 2003).

The growth rate of a central mass (i.e. a collisionless concentration, not a true black hole) from a reservoir of radial orbits is zero if there is a true steady state. However in a state of self-similar virialisation we can expect them to settle into a bulge as they become trapped by the increasing mass. The growth rate is not zero if the central mass is a black hole, since then the outward bound radial orbits are suppressed. In that case however the steady state is only an approximation, except in an infinite system. for a finite system the true timescale would be the free-fall time of the bulk of the accreting mass.

One is inclined not to take these growth estimates seriously, since they simply assume an endless supply of radial particles, and hence an arbitrarily filled loss cone. In fact the radial alignment required to hit a growing black hole from a few hundred parsecs is at least one part in 10^8 to 10^{10} depending on the mass of the black hole! This suggests that instead (MacMillan & Henriksen 2003, see for e.g.) the actual growth involving radial orbits may be by way of a multi-stage process. In the first stage, radial orbits accrete from the galactic halo to form a bound spherical bulge of intermediate size, due to finite angular momentum about the centre (MacMillan & Henriksen 2003). They are trapped there either by the usual mechanism of self-similar infall as the potential increases in time with increasing internal mass, or by dissipative interactions. If there is substructure in the collisionless matter (e.g. stars and dark matter clumps), then these are able to produce dissipational collisions. Ultimately these collisions and tidal interactions can lead to a more gradual growth of a more central mass (MacMillan & Henriksen 2003, for e.g., in the Carnegie meeting).

Recently a high resolution study (Stadel et al 2009) of sub-structure in an isolated halo revealed that this sub-structure disappears in the inner few parsecs. this coincides with the region where the halo is becoming spherical and

where the density power-law is flattening to less than 1. Hence the interactions leading to the sub-structure disappearance may well lead to relaxation.

In addition the radial orbit instability can lead to the development of a bar (MWH 2006). This bar can then transport angular momentum away from the bulge by the ejection of particles. Such ‘interrupted accretion’ may repeat several times on the way to the actual central object. The rapid radial accretion of a bulge is in fact the way in which dark matter halos are thought to grow (Zhao et al., 2003; Lu et al. 2006) initially. This is then followed by a slower growth phase. The DF (31) can be used to describe the environment of the central mass on each scale of the interrupted cascade.

In this connection we refer to the work of Mutka (Mutka 2009) on gravitationally lensed galaxies with double images. He concludes that there are two classes of density cusps with the larger sample (about 80%) showing a logarithmic density slope of ≈ -1.95 well inside the NFW scale radius. The other 20% show this slope as ≈ -1.45 . These may be unresolved triple image lens and ,if so, the measured value should be rejected.

Mutka’s result is a measure of the total mass distribution rather than just the dark matter. Perhaps we are seeing enhanced relaxation in the mixture of stars and dark matter, that leads towards an isothermal cusp, rather than the shallower cusps of the dark matter simulations. It is significant that this inverse square slope is also frequently found by direct dynamical modeling of galaxies (van der Marel 2009).

However an inverse square slope is not restricted to a system of purely radial orbits as the isotropic isothermal distribution shows. In a subsequent paper we survey anisotropic distribution functions in spherical spatial symmetry that also have a self-similar memory. Some of these also provide an inverse square density profile.

The significance of the hierarchy of co-evolving structures is that there will always be a mass correlation between them. Thus if the mass concentration derives its ultimate mass M_\bullet from a halo of radius r_h , while r_s encloses the mass that forms the ultimate bulge mass M_s then

$$\frac{M_\bullet}{M_s} = \frac{r_h}{r_s}. \quad (38)$$

This assumes the pure inverse square density law, which might in fact have a logarithmic correction. In the subsequent paper, we shall find a slightly more general correlation that involves the self-similar memory. Taken at face value this simple relation gives $r_h/r_s \approx 100$.

6 CONCLUSIONS

We have attempted in this paper to find causal reasons for distribution functions that contain a central point mass, or at least a dominant central mass concentration. The particle distribution is confined to particles on radial orbits. Our method was to compare analytic steady state and dynamically developing distribution functions to the results of simulations. In almost every case a self-similar memory was assumed.

The rigorously steady, self-similar steady state ($a \neq 1,18$) does not lend itself to an embedded mass concentration. A central mass is allowed exactly only in the Keplerian

limit wherein $a = 3/2$. This case gives a massless bulge with $\rho \propto r^{-3}$. This is naturally iterated to give an inner flattening, but continued iteration is effectively in powers of $\ln r$.

However, since the inferred particle density based on the steady distribution function is linear in the potential, a non-self-similar solution may be found that does tend to a point mass potential near the centre. The consequent central density profile is too steep however to fit observations of Sagittarius A*, but the larger scale profile is a better fit to simulated density profiles. An iterative procedure starting with a point mass potential yields flattening logarithmic corrections to an r^{-3} profile. The iteration can not be used close to the centre of the system, but the central mass may be ‘renormalised’ to a dominant central mass concentration. This allows a description of the ‘halo region’ around a central bulge that agrees with previous results. Radial orbits are likely to be more realistic as the scale increases.

A shell code and a full N-body study each confirmed the development of the Henriksen and Widrow DF (18, HWDF) in a strictly steady state occupied principally by particles at high binding energy (subject to an eventual numerical cut-off). The special case where the self-similar index $a = 1$ and no assumed steady state was shown to lead to the Fridman and Polyachenko distribution function (FPDF). The FPDF was found to describe accurately the purely radial simulations of isolated collisionless halos carried out in (MacMillan 2006). These simulations retained cosmological initial conditions although non-radial forces were switched off. The final state is close to self-similar virialisation since the infall continues and memory of the initial state is lost. These correspondence between the theory and the simulations allow us some confidence in the distribution functions that we found by remaining ‘close’ to self-similarity.

We may embed a central mass exactly in the FPDF. The density profile retains the r^{-2} behaviour, but the radial velocity dispersion would reflect the variation of the total potential. Thus it decreases as r^{-1} near the central mass, and then decreases logarithmically with r until the moving boundary of the self-similarly virialised state is reached. Realistically the central mass is unlikely to be a true black hole, at least in the early stages of the growth of a galaxy where radial accretion onto the centre is unlikely. The FPDF system may represent a large central mass concentration or ‘bulge’ in an early stage. The growth time of such a central mass in a system of radial orbits is simply proportional to t (measured from the onset of self-similar virialization) so that this would be a relatively rapid phase. Subsequently, with the rise of dissipation and instabilities in the bulge, there may be a slower phase of radial accretion towards the centre. It is possible that this cycle could repeat several times in a process we have referred to as ‘interrupted accretion’. Under this process the r^{-2} density law would apply almost everywhere, although its amplitude would be reset in the different stages. This allows us to expect that the bulge from which a central black hole is fed self-similarly would have a mass proportional to the black-hole mass.

Our final result concerning a rigorously steady system of radial orbits also concerned the special case $a = 1$. We give the deduction of the distribution function because it was omitted elsewhere. It also emphasizes the difference between the self-similar virialised system with continuing infall and the rigorously steady virialised system that is infinite in

extent. The exact DF is a Gaussian that has been associated previously with self-similarity by coarse graining. The assumption of coarse-grained self-similarity has been argued previously to be a more restricted way of reaching the original conclusion of Lynden-Bell (ibid).

This concludes our exploration of reasonable distribution functions comprised of particles on radial orbits that interact collectively to establish self-similarity. In the next paper in this series (II), we shall extend the exploration of self-similarity to include velocity space anisotropies in spherical symmetry.

7 ACKNOWLEDGEMENTS

RNH acknowledges the support of an operating grant from the Canadian Natural Sciences and Research Council. The work of MLeD is supported by CSIC (Spain) under the contract JAEDoc072, with partial support from CICYT project FPA2006-05807, at the IFT, Universidad Autonoma de Madrid, Spain

REFERENCES

- Amorisco, N.C., & Evans, N.W., 2010, arxiv1009.1813A.
Bahcall, J., & Wolf, R.A., 1976, ApJ, 209, 214.
Bertschinger, E., 1985, ApJS, 58, 39.
Bicknell, G.V. & Henriksen, R.N., 1979, ApJ, 232,670.
Binney, J. & Tremaine, S., 1987. *Galactic Dynamics*, Princeton University Press, Princeton, New Jersey.
Carter, B. & Henriksen, R.N., 1991, J. Math. Phys., 32, 2580.
Diemand, J., Kuhlen, M. & Madau, P., 2006, ApJ, 667,859.
Ferrarese, L., & Merritt, D., 2000, ApJ, 539, L9.
Fillmore, J. A., & Goldreich, P., 1984, ApJ, 281, 1.
Fridman, A.M., & Polyachenko, V.L., 1984, *Physics of Gravitating Systems*, Springer, New York.
Fujiwara, T., 1983, PASJ, 35, 547.
Gebhardt, K., et al., 2000, ApJ, 539, L13.
Gillissen, S., et al., 2009, ApJ, 692, 1075.
Henriksen, R.N., Widrow, L.M., 1995, MNRAS, 276, 679.
Henriksen, R.N., Widrow, L.M., 1999, MNRAS, 302, 321.
Henriksen, R.N., & Le Delliou, M., 2002, MNRAS, 331, 423.
Henriksen, R.N., 2004, MNRAS, 355, 1217.
Henriksen, R.N., 2006, MNRAS, 366, 697.
Henriksen, R.N., 2006, ApJ, 653, 894.
Henriksen, R.N., 2007, ApJ, 671, 1147.
Henriksen, R.N., 2009, ApJ, 690, 102.
Kurk, J.D., et al., 2007, ApJ, 669, 32.
Kormendy, J., & Richstone, D., 1995, Ann.Rev.A&A.
Kormendy, J., & Bender, R., 2009, ApJ, 691, L142.
Le Delliou, M., Henriksen, R.N., & MacMillan, J.D., 2009, submitted [arXiv : 0911.2232] (I)
Le Delliou, M., Henriksen, R.N., & MacMillan, J.D., 2009, accepted in A&A [arXiv : 0911.2234] (II)
Le Delliou, M., Henriksen, R.N., & MacMillan, J.D., 2009, accepted in A&A [arXiv : 0911.2238] (III)
Le Delliou, M., 2001, PhD Thesis, Queen’s University, Kingston, Canada.
Lu, Yu, 2006, MNRAS, 368, 193.
Lynden-Bell, D., 1967, MNRAS, 36, 101.
MacMillan, J.D., & Henriksen, R.N., 2002, ApJ, 569, 83.
MacMillan, J.D., & Henriksen, R.N., 2003, Carnegie Observatories Astrophysics Series, 1, *Co-evolution of Black Holes and Galaxies*, L.C. Ho (ed.).

- MacMillan, J., 2006, PhD Thesis, Queen's University at Kingston, ONK7L 3N6, Canada.
- MacMillan, J.D., Widrow, L.M., & Henriksen, R.N., 2006, *ApJ*, 653, 43.
- Magorrian, J., et al., 1998, *AJ*, 115, 2285.
- Maiolino, R., et al., 2007, *A&A*, 472, L33.
- Merritt, D., & Szell, A., 2006, *ApJ*, 648, 890.
- Mutka, P., 2009, Proceeding of *Invisible Universe*, Palais de l'UNESCO, Paris, ed. J-M Alimi.
- Peirani, S. & de Freitas Pacheco, J.A., 2008, *Phys. Rev. D*, 77 (6), 064023.
- Nakano, T., Makino, M., 1999, *ApJ*, 525, L77.
- Navarro, J.F., Frenk, C.S., White, S.D.M., 1996, *ApJ*, 462, 5
- Peebles, P.J.E., 1972, *Gen.Rel.Grav.*, 3, 63.
- Quinlan, G.D., Hernquist, L., Sigurdsson, S., 1995, *ApJ*, 440, 554.
- Stadel, J. et al., 2009, *MNRAS*, 398, L21.
- Van den Bosch, R.C.E., et al., 2008, *MNRAS*, 385, 647.
- van der Marel, R., 2009, in *Unveiling the Mass*, Queen's U., Kingston, Ontario, ed. S. Courteau.
- Young, P., 1980, *ApJ*, 242, 1232.
- Zhao, D.H. et al., 2003, *MNRAS*, 339, 12.
- Walter, F., et al., 2009, *Nature*, 457, 699.